HHS Public Access

Author manuscript

Nat Chem Biol. Author manuscript; available in PMC 2017 April 01.

Published in final edited form as:

Nat Chem Biol. 2016 October ; 12(10): 770–772. doi:10.1038/nchembio.2144.

A hybrid polyketide-nonribosomal peptide in nematodes that promotes larval survival

Qingyao Shou[†], **Likui Feng**[†], **Yaoling Long**, **Jungsoo Han**, **Joshawna K. Nunnery**, **David H. Powell**, and **Rebecca A. Butcher**[*]

Department of Chemistry, University of Florida, Gainesville, FL 32611

Abstract

Polyketides and nonribosomal peptides are two important classes of natural products that are produced by many species of bacteria and fungi, but are exceedingly rare in metazoans. Here, we elucidate the structure of a hybrid polyketide-nonribosomal peptide from *Caenorhabditis elegans* that is produced in the CAN neurons and promotes survival during starvation-induced larval arrest. Our results uncover a novel mechanism by which animals respond to nutrient fluctuations to extend survival.

Polyketides and nonribosomal peptides represent two of the most important classes of natural products used in modern medicine. They include avermectin, whose derivative ivermectin is used to treat parasitic worms in over 300 million people annually, the antibiotic vancomycin, which is used to treat life-threating infections by gram-positive bacteria, and the immunosuppressant FK506, an essential drug after organ transplantation[1]. These natural products are biosynthesized by polyketide synthases (PKSs) and nonribosomal peptide synthetases (NRPSs), modular megasynthases that function in either an assembly-line or iterative manner[2]. Although PKS and NRPS genes are commonly found in many bacterial and fungal species, only simple, single-module PKSs and NRPSs are present in a few animal species[3,4]. Thus, it is quite remarkable that the genome of the nematode *C. elegans* encodes a huge (865 kDa), multi-module hybrid PKS/NRPS on the X chromosome (PKS-1) and a large (333 kDa), multi-module NRPS on chromosome III (NRPS-1)[5,6]. Homologs of PKS-1 and NRPS-1 are present in most nematode species, including parasitic ones (Supplementary Results, Supplementary Fig. 1)[5]. Here, we elucidate the chemical structure of the polyketide-nonribosomal peptide produced by PKS-1/NRPS-1 and show that this natural product promotes recovery from and survival during starvation-induced larval arrest.

[*]Correspondence to: butcher@chem.ufl.edu.
[†]equal contributions

Author Contributions

Q.S. purified and structurally characterized the nemamides. L.F. generated transgenic worm strains and performed biological assays. Y.L. performed metabolomic analyses. J.H. generated extracts. J.K.N. analyzed nemamide stability. Q.S., L.F., Y.L., D.H.P., and R.A.B. analyzed the data. R.A.B., Q.S., and L.F. wrote the manuscript.

Competing Financial Interests

The authors declare no competing financial interests.

We used comparative, untargeted metabolomics to identify the masses of the natural products that PKS-1 and NRPS-1 produce. Extracts from worms and from conditioned culture medium were generated from mixed-stage cultures of wild-type worms, *pks-1* mutant worms, and *nrps-1* mutant worms. The metabolites in the extracts were analyzed by HR-LC-MS and compared using XCMS (Fig. 1a,b)[7]. Two peaks (*m/z* 757.3866 and 755.3700), termed nemamide A (**1**) and nemamide B (**2**), respectively, were present in wild-type worm extracts and completely absent in *both* mutant worm extracts (Supplementary Fig. 2). Thus, PKS-1 and NRPS-1 likely work together to make a hybrid polyketide-nonribosomal peptide. Nemamide A and B are associated with the worm body rather than secreted into the culture medium, as the molecules were not detected by HR-LC-MS in the culture medium extracts.

To purify enough of the nemamides to identify their structures by NMR spectroscopy, wild-type worms were grown in an axenic, semi-defined medium[8] that gives a much higher density of worms than bacteria-fed worm cultures. We grew ~50L of worm culture, and ultimately, we estimate that we purified only ~70 μg of nemamide A and less of nemamide B. These compounds were extracted from freeze-dried worms and purified using a short silica gel column, followed by an HP-20 column, a Sephadex LH-20 column, and then HPLC. The extraction and purification process had to be completed for small batches of worms (from ~2L of culture) within 1–2 days to prevent degradation of the nemamides. The exact masses of nemamide A and B indicated the molecular formulas $C_{34}H_{54}N_8O_{10}$ and $C_{34}H_{52}N_8O_{10}$, respectively. NMR spectra, including dqf-COSY, TOCSY, HSQC, HMBC, and ROESY spectra, were obtained for nemamide A and used to determine its molecular connectivity (Supplementary Table 1, Supplementary Fig. 3 and 4).

Marfey's method[9] was used to establish that nemamide A contains one L-Asn and two D-Asn (**Online Methods**). The relative configurations of the six stereocenters in nemamide A were determined using coupling constants and ROESY correlations (Supplementary Figs. 5–7). The absolute configurations of the four stereocenters in the macrolactam ring were determined by chemically synthesizing three model cyclic peptides with the three possible configurations (2*S*,6*R*,10*R*,18*R*, 2*R*,6*S*,10*R*,18*S*, and 2*R*,6*R*,10*S*,18*S*) and comparing their NMR spectra to that of nemamide A (Supplementary Fig. 8, Supplementary Tables 2 and 3). Additional support for the absolute configurations of the stereocenters at C-20 and C-22 was obtained through comparison of the observed CD spectrum of nemamide A to a predicted CD spectrum (Supplementary Fig. 9). Additional support was also provided by analysis of the ketoreductase (KR) domain responsible for installing the C-22 stereocenter (see discussion of biosynthesis below). Thus, we propose that the absolute configuration of nemamide A is 2*S*,6*R*,10*R*,18*R*,20*R*,22*S* (Fig. 1c). In comparison to nemamide A, nemamide B has one additional double bond, based on its NMR spectra, HR-MS, MS/MS, and UV spectrum (Fig. 1c, Supplementary Fig. 10–12).

Although the nemamide structures could not be predicted from the protein sequences of PKS-1 and NRPS-1, they are largely consistent with the domain architectures of the megasynthases. Biosynthesis begins on PKS-1, which initially extends the growing natural product through six iterative cycles, then uses two additional PKS modules to further extend the polyketide in an assembly-line manner, and then uses the C-terminal NRPS module to

incorporate β-Ala (Fig. 1d). Next, the growing natural product is passed to NRPS-1, which sequentially adds D-Asn, D-Asn, and L-Asn and then forms the macrolactam ring (Fig. 1d). The biosynthetic pathway, however, has several non-canonical features, including (1) KR domains (specifically, KR_2 and KR_3) that cannot be classified as A-type or B-type, which would enable their stereospecificities to be predicted (Fig. 1d, Supplementary Fig. 13)[10], (2) Missing enzymatic domains, such as methyltransferase and aminotransferase domains, that are likely encoded elsewhere in the *C. elegans* genome (Fig. 1d)[11], (3) Adenylation domains with protein sequences that diverge significantly from those of bacterial and fungal adenylation domains (Fig. 1d, Supplementary Table 4)[12], (4) The absence of any obvious epimerase domains[2] despite the presence of D-Asn in the nemamides (Fig. 1d), and (5) A chain-terminating thioesterase domain present not only at the C-terminus of NRPS-1, but also, unusually, at the C-terminus of PKS-1 (Fig. 1d, Supplementary Figs. 14 and 15)[2,13].

Using transcriptional reporter strains, we showed that *pks-1* and *nrps-1* are expressed during all larval stages and the adult stage specifically in the CAN neurons, two essential neurons with a poorly defined role that extend the length of the worm and are closely associated with the excretory canals (Fig. 2a,b)[14]. Given that *pks-1* and *nrps-1* are expressed neuronally, we speculated that the nemamides might play a signaling role in development. With sufficient food (bacteria), *C. elegans* will progress from the egg, through four larval stages (L1–L4) to the adult. However, if *C. elegans* eggs hatch to L1 larvae in the complete absence of food, the L1 larvae will arrest, but then resume development upon addition of food[15]. The *pks-1* and *nrps-1* arrested L1s recovered much slower than wild-type arrested L1s when placed on food (Fig. 2c). The mutants progress from the egg to the L4 stage at the same rate as wild-type worms (Supplementary Fig. 16), and thus, do not have a general defect in larval progression or development, but rather a specific defect in recovery from L1 arrest. Additionally, the *pks-1* and *nrps-1* mutants enter and recover from the dauer larval stage as well as wild type (Supplementary Fig. 17). Like wild-type worms, the *pks-1* and *nrps-1* mutants maintain proper somatic progenitor cell and germline arrest during L1 arrest (Supplementary Fig. 18 and 19). Thus, although the *pks-1* and *nrps-1* mutants are defective in recovery from L1 arrest, they are not defective in L1 arrest initiation and maintenance[16].

The insulin/IGF-1 pathway is an important regulator of L1 arrest and recovery, and specific insulins are down-regulated upon L1 arrest and then up-regulated following food addition[15,17,18]. To determine whether the nemamides affect insulin expression, we profiled the expression of all 40 *C. elegans* insulins by qRT-PCR during L1 arrest and recovery. In the *pks-1* and *nrps-1* arrested L1s, *ins-4*, *ins-5*, *ins-19*, and *ins-37* are expressed at higher levels than in wild-type arrested L1s (Supplementary Fig. 20). Furthermore, unlike in wild type, in the *pks-1* and *nrps-1* backgrounds, *ins-5* and *ins-19* are not induced during L1 recovery and *ins-4* and *ins-37* are down-regulated during L1 recovery (Fig. 2d, Supplementary Fig. 21). The production of the nemamides decreases during L1 recovery (Supplementary Fig. 22). Thus, our data suggest that the nemamides are negative regulators of the expression of specific insulins, such that expression of these insulins increases as nemamide levels decrease during L1 recovery.

The *pks-1* and *nrps-1* mutants show reduced survival during prolonged L1 arrest (Fig. 2e, Supplementary Fig. 23). Although it has been shown that L1 survival is density-dependent

and that L1s secrete unidentified small molecules that increase survival[19], the nemamides are unlikely to be a component of this pheromone, since the mutants showed reduced survival relative to wild type, regardless of worm density (Supplementary Fig. 24). *C. elegans* mutants which eat less display reduced survival during L1 arrest[15]. However, the *pks-1* and *nrps-1* mutants are not defective in bacterial food consumption or pharynx pumping (Supplementary Figs. 25 and 26), and thus, their reduced survival is not simply due to reduced nutrient stores. Because the insulin/IGF-1 pathway regulates L1 survival, we investigated the genetic interactions between this pathway and the nemamide pathway. Performing the survival assay in insulin/IGF-1 pathway mutant backgrounds suggests that although nemamide signaling regulates insulin expression, it functions at least partially independently of the insulin/IGF-1 pathway (Fig. 2e, Supplementary Fig. 27)[15].

The mechanisms by which animals control their development and physiology in response to nutrient fluctuations are poorly understood. The nemamides could potentially serve as a chemical tool with which to dissect this process. We show that the nemamides are important for survival during and recovery from starvation-induced larval arrest. The nemamides likely influence larval development in *C. elegans* in part by modulating insulin signaling (Supplementary Fig. 28). The nemamides represent the first polyketide-nonribosomal peptides biosynthesized in an assembly-line manner in a metazoan. Their discovery will enable the exploration of polyketide and nonribosomal peptide biosynthesis in the context of a complex animal system. Nemamide biosynthesis likely requires additional enzymes that act in *trans*. Future studies of the site of expression and regulation of these enzymes could potentially provide additional insights into the biological role and site of action of the nemamides. As the nemamide biosynthetic genes are found in most nematode species, including parasitic ones, the role of the nemamides in larval development is likely conserved across nematode evolution.

Online Methods

Strains and culture methods

Worms were maintained on *E. coli* OP50 according to standard methods. Strains used in this study include wild type (N2), *pks-1(ttTi24066)*, *pks-1(ok3769)* (this allele was only used in Supplementary Fig. 23), *nrps-1(ttTi45552)*, *pks-1(ttTi24066); nrps-1(ttTi45552)*, *ayIs7*[*hlh-8p::gfp*], *pks-1(ttTi24066); ayIs7*, *nrps-1(ttTi45552); ayIs7*, *unc-31(e928)*, *unc-31(e928); pks-1(ttTi24066)*, *unc-31(e928); nrps-1(ttTi45552)*, *daf-16(mu86)*, *daf-16(mu86); pks-1(ttTi24066)*, and *daf-16(mu86); nrps-1(ttTi45552)*. The *pks-1(ttTi24066)*, *nrps-1(ttTi45552)*, and *pks-1(ok3769)* strains were backcrossed two, four, and four times, respectively. The double mutants were constructed from single mutants using standard genetic methods and the presence of alleles was verified by PCR (Supplementary Table 5).

Generation of worm extracts for metabolomic analysis

The wild-type, *pks-1,* and *nrps-1* strains were each grown at room temperature on two NGM agar plates (10 cm) spread with 0.75 mL 25X OP50 until the food on the plates was almost gone. Then, the worms were transferred to 1 L Erlenmeyer flasks containing S medium (350

mL). The worm cultures were grown at 22.5°C for 3 d and were fed with 3.5 mL of 25X OP50 every day. For sample collection, the culture flasks were placed in an ice-bath for 30 min to 1 h to settle the worms. Then, the worms were transferred from the bottom of the flasks to a 50 mL centrifuge tube and were centrifuged (1000 rpm for 5 min) to separate the worms from the worm medium. After the centrifugation, the supernatant was combined with the worm medium. The process was repeated until most of the worms were removed from the flasks. The collected worms were washed with water three times and centrifuged (1000 rpm for 5 min), and then they were soaked in 10 mL of water for 1 h in a shaking incubator (22.5°C, 225 rpm) to remove bacteria from their digestive tract. The worms were collected by centrifugation and were freeze-dried. The dried worm pellets were ground with sea sand (2 g sand per 800–900 mg dried worms) using a mortar and pestle. The ground worms were extracted with 50 mL of ethanol for 1 h, and the extract was filtered through filter paper. The fitrate was collected and dried using a rotovap. The collected worm medium was filtered using Celite and then using a 0.2 μm filter. The medium was extracted with ethyl acetate, and the ethyl acetate layer was then dried using a rotovap. The dried worm and worm media samples were each resuspended in 125 μL of 50% (vol/vol) ethanol in water, sonicated (if needed), and centrifuged (15000 rpm for 1 min) before analysis by HR-LC-MS. In later experiments to attempt to detect the nemamides in culture medium, the culture medium was instead freeze-dried and extracted with 190 proof ethanol.

General methods for chemical analysis

HR-LC-MS analysis was performed on an Agilent 1200 high performance liquid chromatography (HPLC) system equipped with a UV-Vis diode array detector and a 6220 TOF MS using positive ESI in both profile and centroid modes. NMR spectra were recorded on a Varian INOVA 600 equipped with a 1.5 mm microcryoprobe[22], except for an additional HMBC spectrum of nemamide A, which was recorded on a Bruker Avance 800 spectrometer equipped with a 1.7 mm microcryoprobe (Supplementary Fig. 3i). CD spectra were obtained on an AVIV-202 CD spectrometer.

Metabolomic analysis

The worm and conditioned medium samples for each worm strain (N2, *pks-1*, and *nrps-1*) each consisted of three biological replicates and two technical replicates. 5 μL of each sample was injected. LC separation was achieved on two Onyx Monolithic C_{18} (Phenomenex, 100 × 4.6 mm, 5 μm) columns in series using a solvent gradient of 1% acetic acid in water (solvent A) and 1% acetic acid in acetonitrile (solvent B) at a flow rate of 0.33 mL / min. The solvent flow was maintained at 5% B for 6.5 min, then ramped to 100% B over 19 min, then maintained at 100% B for 9.5 min, then ramped to 5% B over 10 min, and maintained at 5% B for 5 min. The mass spectrometer settings include a drying gas flow of 10 L / min, a gas temperature of 325 °C, a nebulizer pressure of 50 psi, a capillary voltage of 4000 V, a fragmentor voltage of 180 V, and a skimmer voltage of 60 V. Worm samples were run in a random order to minimize the impact of mass or retention time shift on the analyses. Data files were converted to mzXML format in centroid mode using ProteoWizard software[23]. Metabolomic comparisons were performed using XCMS Online[7] using the default parameters for HPLC-Q-TOF, except that the “Matched Filter” feature detection

method and the “Peak Groups” retention time correction method (with nonlinear alignment) were used.

Purification and characterization of nemamides

Wild-type worms were shaken at 225 rpm for 7 d at 22.5 °C in 2.8 L baffled flasks containing 500 mL of CeHR medium[8] with 20% cow’s milk. Worms were collected by centrifugation, washed with water, shaken in water for 30 min to clear their intestines, and washed again with water. Worms were stored frozen at −20 °C until needed. For extraction and fractionation process, worms from 2 L-worth of culture were processed at a time. After freeze drying, worms were ground for 15 min with 70 g of sand using a mortar and pestle. The pulverized worms were transferred to a 1 L Erlenmeyer flask, and 700 mL of 190 proof ethanol was added to the flask. The flask was shaken at 300 rpm for 3.5 h. The extract was filtered using a Buchner funnel and filter paper and evaporated with a rotovap at 27 °C. The extract was then subjected to silica gel chromatography and eluted with a gradient of ethyl acetate/methanol (1:0, 9:1, 1:1, 0:1) to give four fractions (A – D). Fraction D was evaporated with a rotovap at 27 °C, redissolved in 12 mL of methanol, and centrifuged at 3500 rpm for 10 min. The supernatant was dried and dissolved in 10 mL 70% methanol/water. Fraction D was then applied to an HP-20 column, eluting with MeOH/H2O (7:3 to 9:1) to give four subfractions (D1 – D4). Subfraction D3 was applied to a Sephadex LH-20 column, eluting with methanol to give seven subfractions (D3a – D3g). Fraction D3g, which contained both nemamide A and B based on LC-MS analysis, was further fractionated by HPLC (eclipse XDB-C_{18} column, 150 × 4.6 mm, 5 μm), using a gradient of methanol and water (ramping from 10% to 100% methanol over 30 min, holding at 100% methanol for 6 min, then returning to 10% methanol over 4 min; flow rate 1 mL / min; UV detection at 280 nm), to obtain purified nemamide A and B. Nemamide A: For NMR spectra and ^{1}H and ^{13}C NMR data of nemamide A, see Supplementary Figure 3 and Supplementary Table 1; UV (methanol): λ_{max} 258, 269, 279 nm; HR-ESIMS (*m/z*): $[M+Na]^+$ calcd. for $C_{34}H_{54}N_8O_{10}Na$ 757.3861, found 757.3866. Nemamide B: For NMR spectra, see Supplementary Figure 12; UV (methanol): λ_{max} 286, 301, 315 nm; HR-ESIMS (*m/z*): $[M+Na]^+$ calcd. for $C_{34}H_{52}N_8O_{10}Na$ 755.3704, found 755.3700.

Marfey’s analysis

Nemamide A (purified from worms from 2.5 L of culture) was hydrolyzed with 200 μL of 6 N HCl at 110 °C for 12 h. The reaction was then dried down by rotovap, and the residue was dissolved in 50 μL of water. 50 mM stock solutions of the amino acid standards (L-Asp, D-Asp, L-Asn, D-Asn) were made in water. 20 μL of 1 M $NaHCO_3$ and 100 μL of 1-fluoro-2,4-dinitrophenyl-5-L-alaninamide (L-FDAA, Marfey’s reagent; 1% w/v in acetone) were added to 50 μL of the sample or the amino acid standards. After heating at 37 °C for 60 min, reactions were quenched by addition of 20 μL of 1 N HCl. The sample reaction was diluted with 100 μL of acetonitrile while the reactions of the amino acid standards were diluted with 810 μL of acetonitrile. The reactions of the sample and standards were subjected to LC-MS analysis (Phenomenex Luna $C_{18,}$ 4.6 × 100 mm, 5 μm) using a linear gradient of water with 0.1% formic acid and acetonitrile with 0.1% formic acid (holding at 10% acetonitrile for 5 min, then ramping to 50% acetonitrile over 30 min; flow rate, 0.7 mL/min; UV and ESI-MS detection, 340 nm and negative ion mode). Analysis with both Asn

and Asp amino acids indicated the conversion of Asn to Asp during the acid hydrolysis step for both the sample and the Asn amino acid standards. Retention times for L-FDAA-L-Asp and L-FDAA-D-Asp were 22.0 and 22.7 min, respectively. The extracted ion chromatogram (*m/z* 384) for the sample indicated the presence of L-FDAA-L-Asp and L-FDAA-D-Asp in a 1:2.16 ratio.

Cyclic peptide synthesis

H-β-Ala-2-ClTrl resin was purchased from Novabiochem, and Fmoc-L-Asn(Trt)-OH, Fmoc-D-Asn(Trt)-OH, (*R*)-3-(Fmoc-amino)butyric acid, and (*S*)-3-(Fmoc-amino)butyric acid were purchased from Chem-Impex International. Compound **3** was made through the sequential coupling to the resin of (*R*)-3-(Fmoc-amino)butyric acid, Fmoc-L-Asn(Trt)-OH, Fmoc-D-Asn(Trt)-OH, and Fmoc-D-Asn(Trt)-OH, followed by cleavage from the resin and cyclization. Compound **4** was made through the sequential coupling to the resin of (*S*)-3-(Fmoc-amino)butyric acid, Fmoc-D-Asn(Trt)-OH, Fmoc-L-Asn(Trt)-OH, and Fmoc-D-Asn(Trt)-OH, followed by cleavage from the resin and cyclization. Compound **5** was made through the sequential coupling to the resin of (*S*)-3-(Fmoc-amino)butyric acid, Fmoc-D-Asn(Trt)-OH, Fmoc-D-Asn(Trt)-OH, and Fmoc-L-Asn(Trt)-OH, followed by cleavage from the resin and cyclization. Solid-phase peptide synthesis was conducted in 10 mL BD Luer-Lok syringes. For deprotection, H-β-Ala-2-ClTrl resin (0.25 g, 0.375 mmol/g) was swelled in dry CH_2Cl_2 for 20 min. The resin was treated with 20% (v/v) piperidine / DMF (5 mL) for 30 min and then washed with DMF (3 × 5 mL). For amino acid coupling, a solution of protected amino acid (5 eq.) in DMF, HOBt (5.5 eq.) in DMF and DIC (5.5 eq.) together with 5 mL CH_2Cl_2 was added to the resin. After 4 h, the resin was washed with DMF (5 mL), CH_2Cl_2 (5 mL), and DMF (5 mL). The reaction was monitored using the ninhydrin test. When the ninhydrin test was negative, deprotection and coupling to the next amino acid was carried out. For cleavage of the linear peptide, the resin was treated with a 5 mL solution of 1,1,1,3,3,3-hexafluoro-2-propanol in CH_2Cl_2 (1:4, v/v) for 30 min. This process was repeated two additional times, and the combined cleavage solution was concentrated in vacuum. For cyclization of the linear peptide, the crude linear peptide (100 mg, 0.08 mmol) was dissolved in 80 mL DMF, and 4-(4,6-dimethoxy-1,3,5-triazin-2-yl)-4-methylmorpholinium tetrafluoroborate ($DMTMM^+$ BF_4^-, 54 mg, 0.16 mmol) and iPr_2NEt (28 μL, 158.6 μmol) was added to the solution. The solution was stirred overnight and then concentrated under reduced pressure using a rotovap. For deprotection of the trityl groups, 10 mL of a solution of TFA, triisopropylsiline, and water (95:2.5:2.5, v/v/v) was added for 2 h, and then concentrated to give the crude cyclic peptide. For purification of the cyclic peptide, the crude cyclic peptide was initially purified on a C_{18} column (50g Octadecyl-functionalized silica gel, 3.5 cm × 50 cm), eluted with 10% methanol, and then further purified using reversed-phase HPLC (0–5 min: 2% acetonitrile, 5–15 min: 2%–30% acetonitrile, 15–20 min: 30% acetonitrile) to afford pure cyclic peptide.

Construction of reporter strains

The PEST sequence from pAF207[20] (gift of Alison Frand) was subcloned into pPD114.108 at the XhoI/EcoRI sites to generate pPD114.108-*gfp::pest*. 4.563 kb of the *pks-1* promoter and 3 kb of the *nrps-1* promoter were amplified from *C. elegans* genomic DNA (Supplementary Table 5). The *pks-1* and *nrps-1* promoters were inserted into the SalI/NotI

and AscI/NotI sites, respectively, of pPD114.108 or pPD114.108-*gfp::pest* to obtain *pks-1p::gfp* and *nrps-1p::gfp* or *pks-1p::gfp-pest* and *nrps-1p::gfp-pest*, respectively. For the *canp::mcherry* reporter, the CAN-specific promoter was cut from *canp::yfp*[24] (gift of Nadeem Moghal) at two SphI sites and inserted into pMC10 (a gift of Piali Sengupta). 50 ng/μL of the transgenes, along with 50 ng/μL of the co-injection marker *unc-122p::DsRed* (gift of Piali Sengupta), were injected into wild-type worms. At least three independent transgenic strains were analyzed. Imaging was conducted on a Zeiss Axiovert. A1 microscope equipped with ZEN lite 2012 camera.

Cyclic peptide 3 (2*S*,6*R*,10*R*,18*R*)

^{1}H NMR (600 MHz, dimethyl sulfoxide-d_6) δ 8.63 (brs, 10-NH), 8.20 (brd, $J_{6,6\text{-NH}}$ = 8.8 Hz, 6-NH), 7.80 (brs, 8-NH_2b), 7.49 (brd, $J_{2,2\text{-NH}}$ = 8.1 Hz, 2-NH), 7.43 (brs, 12-NH_2b), 7.36 (brs, 15-NH), 7.32 (brs, 8-NH_2a), 7.11 (brs, 4-NH_2b), 6.96 (brs, 12-NH_2a), 6.95 (brd, $J_{18,18\text{-NH}}$ = 7.9 Hz, 18-NH), 6.82 (brs, 4-NH_2a), 4.48 (m, H-2), 4.41 (m, H-6), 4.25 (m, H-10), 3.96 (m, H-18), 3.42 (m, H-15b), 3.18 (m, H-15a), 2.98 (dd, $J_{7a,7b}$ = 16.4 Hz, $J_{6,7b}$ = 4.7 Hz, H-7b), 2.62 (dd, $J_{3a,3b}$ = 19.3 Hz, $J_{2,3b}$ = 6.5 Hz, H-3b), 2.58 (brd, $J_{7a,7b}$ = 17.2 Hz, H-7a), 2.57 (overlap, H-14b), 2.51 (overlap, H-11a, 11b), 2.46 (overlap, H-17b), 2.43 (dd, $J_{3a,3b}$ = 19.4 Hz, $J_{2,3a}$ = 12.7 Hz, H-3a), 2.42 (overlap, H-14a), 2.15 (brd, $J_{17a,17b}$ = 12.0 Hz, H-17a), 0.98 (d, $J_{18,19}$ = 5.9 Hz, H-19); ^{13}C NMR (125 MHz, dimethyl sulfoxide-d_6) δ 173.6 (C-8, 12), 173.3 (C-13), 171.2 (C-4), 171.1 (C-9), 170.7 (C-16), 170.5 (C-5), 169.7 (C-1), 52.1 (C-10), 49.9 (C-2), 49.2 (C-6), 43.0 (C-18), 41.4 (C-17), 36.8 (C-3), 35.6 (C-11), 35.4 (C-7), 34.8 (C-15), 33.5 (C-14), 20.7 (C-19); ESIMS *m/z* 499.3 $[M+H]^+$, *m/z* 497.3 $[M-H]^-$.

Cyclic peptide 4 (2*R*,6*S*,10*R*,18*S*)

^{1}H NMR (600 MHz, dimethyl sulfoxide-d_6) δ 8.39 (brd, $J_{10,10\text{-NH}}$ = 7.4 Hz,10-NH), 7.92 (brs, 8-NH_2b), 7.85 (brd, $J_{2,2\text{-NH}}$ = 8.8 Hz, 2-NH), 7.81 (brd, $J_{6,6\text{-NH}}$ = 8.8 Hz, 6-NH), 7.47 (brs, 8-NH_2a), 7.38 (brs, 4-NH_2b), 7.33 (brs, 12-NH_2b), 7.25 (brs, 15-NH), 7.08 (overlap, 18-NH), 6.95 (brs, 12-NH_2a), 6.85 (brs, 4-NH_2a), 4.49 (m, H-2), 4.46 (m, H-10), 4.40 (m, H-6), 3.97 (m, H-18), 3.55 (overlap, H-15b), 3.14 (overlap, H-15a), 3.05 (dd, $J_{7a,7b}$ = 17.2 Hz, $J_{6,7b}$ = 3.8 Hz, H-7b), 2.69 (dd, $J_{3a,3b}$ = 15.8 Hz, $J_{2,3b}$ = 5.6 Hz, H-3b), 2.65 (dd, $J_{11a,11b}$ = 15.7 Hz, $J_{10,11b}$ = 6.8 Hz, H-11b), 2.54 (overlap, H-7a), 2.51 (overlap, H-17b), 2.48 (overlap, H-11a, 14b), 2.43 (dd, $J_{3a,3b}$ = 15.8 Hz, $J_{2,3a}$ = 6.9 Hz, H-3a), 2.36 (m, H-14a), 2.11 (brd, $J_{17a,17b}$ = 11.3 Hz, H-17a), 0.97 (d, $J_{18,19}$ = 5.9 Hz, H-19); ^{13}C NMR (125 MHz, dimethyl sulfoxide-d_6) δ 173.8 (C-8), 172.6 (C-13), 172.3 (C-12), 171.8 (C-4), 170.3 (C-5), 170.2 (C-9, 16), 169.6 (C-1), 49.7 (C-2), 49.3 (C-10), 48.7 (C-6), 43.1 (C-18), 41.5 (C-17), 35.4 (C-11), 35.3 (C-7), 35.1 (C-3), 34.7 (C-14), 34.3 (C-15), 20.9 (C-19); ESIMS *m/z* 499.3 $[M+H]^+$, *m/z* 497.2 $[M-H]^-$.

Cyclic peptide 5 (2*R*,6*R*,10*S*,18*S*)

^{1}H NMR (600 MHz, dimethyl sulfoxide-d_6) δ 8.89 (brd, $J_{6,6\text{-NH}}$ = 5.2 Hz, 6-NH), 8.48 (brs, 10-NH), 7.49 (brd, $J_{2,2\text{-NH}}$ = 7.9 Hz, 2-NH), 7.40 (brs, 12-NH_2b), 7.33 (brs, 8-NH_2b), 7.27 (brs, 4-NH_2b), 7.00 (brs, 15-NH), 6.98 (brs, 12-NH_2a), 6.89 (brs, 8-NH_2a), 6.88 (brs, 4-NH_2a), 6.66 (brd, $J_{18,18\text{-NH}}$ = 7.7 Hz, 18-NH), 4.40 (m, H-2, 10), 4.33 (m, H-6), 3.97 (m, H-18), 3.33 (overlap, H-15a,15b), 2.60 (overlap, H-7b), 2.56 (overlap, H-3a, 3b), 2.56

(overlap, H-14b), 2.49 (overlap, H-11b), 2.48 (overlap, H-7a), 2.36 (brd, $J_{17a,17b}$ = 13.1 Hz, H-17b), 2.31 (brd, $J_{11a,11b}$ = 16.1Hz, H-11a), 2.23 (m, H-14a), 2.06 (brd, $J_{17a,17b}$ = 13.0 Hz, $J_{17a,18}$ = 9.4 Hz, H-17a), 1.04 (d, $J_{18,19}$ = 6.5 Hz, H-19); ^{13}C NMR (125 MHz, dimethyl sulfoxide-d_6) δ 173.9 (C-9), 172.3 (C-13), 171.2 (C-4), 170.9 (C-8), 170.7 (C-5), 170.3 (C-12), 170.1 (C-1), 170.0 (C-16), 50.9 (C-2, 6, 10), 42.6 (C-18), 41.7 (C-17), 36.5 (C-3), 35.6 (C-11), 35.4 (C-7, 15), 34.0 (C-14), 20.1 (C-19); ESIMS *m/z* 499.3 $[M+H]^+$, *m/z* 497.3 $[M-H]^-$.

L1 recovery, dauer formation, and dauer recovery assays

For L1 recovery assays, eggs were isolated from well-fed gravid worms using alkaline bleach treatment, diluted to 4–6 eggs/ μL in M9 buffer, and shaken for 24 h at 22.5 °C and 225 rpm. Approximately 80–120 synchronized L1s were placed onto a 3 cm NGM plate with OP50 at 15 °C, 20 °C, or 25 °C. After a certain period of time (40 h at 25 °C, 48 h at 20 °C, and 80 h at 15 °C), the percentage of worms at or passed the L4 stage was determined. For each experiment, five plates were analyzed for each strain, the percentage of worms at or passed the L4 stage was calculated for each plate, and the percentages for each strain were averaged. Dauer formation assays were performed for wild-type, *pks-1*, and *nrps-1* with vehicle control or 1 μM asc-C6-MK at 25 °C as described[26]. Dauer recovery assays were performed by taking dauers from dauer formation assay plates and moving them to a lawn of bacteria for 24 h at 20 °C before scoring for recovery.

Egg to L4 development assay

Worms were maintained at 15 °C, 20 °C, or 25 °C for 2–3 generations. For egg lay assay, L4s were moved onto a new plate one day before the beginning of the experiment, and the next day 8 adults were used to perform a 1 h egg lay for each 3 cm NGM plate with OP50. Alternatively, for egg prep experiment, eggs were isolated from well-fed gravid worms using alkaline bleach treatment, washed, and added to 3 cm NGM plates with OP50. In both egg lay and egg prep assays, eggs were then incubated at 15 °C, 20 °C, or 25 °C, and after a certain period of time (40 h at 25 °C, 48 h at 20 °C and 80 h at 15 °C), the percentage of worms at or passed the L4 stage was determined. For each experiment, five plates were analyzed for each strain, and the percentages for each strain were averaged.

Analysis of expression of insulins using qRT-PCR

Well-fed gravid adults were collected from multiple 10 cm NGM plates and eggs were isolated by using alkaline bleach treatment, diluted to 4–6 eggs / μL in M9 buffer, and shaken for 24 h at 21 °C, 225 rpm. Then 25 mg/mL of OP50 was supplied to initiate recovery. Worms at 0 h and 6 h after feeding were collected by washing with cold M9 buffer, flash-frozen and stored at −80 °C before qRT-PCR. Total RNA extraction, an on-column DNase treatment, and cDNA generation were performed as described[26], except that 0.25 μg of total RNA was used for reverse transcription. All primers for insulin genes were as described[27], except for the ones for *ins-3*, *ins-26*, and *ins-31*, which were as described here[16], and the ones for *ins-11*, which were designed using the Real-time PCR Primer Design Tool (IDT) and are listed in Supplementary Table 5. qPCR was performed using SYBR Green select Master Mix (Life Technologies) on a 7500 Fast Real-Time PCR system (Applied Biosystems) using the standard mode. PCR parameters include a holding stage at

50 °C for 2 min and another holding stage at 95 °C for 5 min, followed by 40 cycles of 95 °C for 10s, 57 °C for 20s and 72 °C for 30s. Relative expression levels for recovered versus arrested L1s were determined using the $\Delta\Delta C_t$ method[28], and normalized to the expression levels of endogenous control genes *act-1*, *pmp-3* and Y45F10D.4[26]. Ratio of relative expression level for each strain was calculated by comparing the relative expression level at 6 h after feeding with the level at 0 h.

Nemamide production

Eggs were isolated from well-fed gravid worms using alkaline bleach treatment, diluted in S basal in a 125 mL flask, and shaken for 24 h at 20 °C and 200 rpm. Then, the synchronized L1s were inoculated into 2.8 L flasks with the density adjusted to 6 L1s / μL in 200 mL S medium (starved L1s) or 190 mL S medium plus 10 mL concentrated OP50 (fed L1s). Starved and fed L1 worms were cultured at 20 °C and 150 rpm for 6 h. L1s were then harvested by washing three times with S basal. L1s were freeze-dried, ground with sand, and extracted with ethanol, as described above, and then the nemamides were analyzed by LC-MS.

M cell division assay

For the *ayIs7[hlh-8p::gfp], pks-1; ayIs7,* and *nrps-1; ayIs7* strains, eggs were isolated from well-fed gravid worms using alkaline bleach treatment, diluted to 4–6 eggs/ μL in M9 buffer with 0.08% ethanol, and shaken for 7d at 22.5 °C and 225 rpm. Worms were examined for M cell division using a fluorescent microscope. > 50 worms were examined for each genotype.

Fertility and brood size upon recovery from L1 arrest

For the wild-type, *pks-1*, and *nrps-1* strains, eggs were isolated from well-fed gravid worms using alkaline bleach treatment, diluted to 4–6 eggs/ μL in M9 buffer, and shaken for 5d at 22.5 °C and 225 rpm. Worms were then moved to a lawn of bacteria, allowed to develop to the L4 stage, and then singled. Survival and fertility were examined 2–3d later.

L1 survival assay

Eggs were isolated from well-fed gravid worms using alkaline bleach treatment, diluted in M9 buffer in a 125 mL flask, and shaken for 24 h at 20 °C and 200 rpm. Then, the density of the synchronized L1s was adjusted to 4–6 L1s / μL (Fig. 2e) or 20–25 L1s / μL (Supplementary Fig. 24, high density) or 0.5–0.8 L1s / μL (Supplementary Fig. 24, low density) in M9 buffer. Every other day, 20 μL starved L1 samples were seeded onto 3 cm NGM plate with OP50 at 20 °C, and three plates were seeded for each strain. The plated worms were scored after 2–3 d, and worms at or passed the L2 stage were scored as surviving worms. For each experiment, three plates were analyzed for each strain, the percentage of surviving worms was calculated for each plate, and the percentages for each strain were averaged. Survival curves in Figure 2e and Supplementary Figure 24 and Supplementary Figure 27 were statistically analyzed as previously described[29].

Pumping assay

At least 30 young adults for each strain (wild-type, *pks-1*, and *nrps-1*) were analyzed while on a lawn of OP50 by counting the number of pharynx pumps per 30s under the dissecting microscope at room temperature.

Phylogeny and domain analysis

Phylogenetic trees were generated in MEGA 6, and domain analysis was performed using antiSMASH 3.0.[30,31] Protein sequences were retrieved from NCBI or Wormbase Parasite.

Supplementary Material

Refer to Web version on PubMed Central for supplementary material.

Acknowledgments

We thank Andy Fire, Alison Frand, Nadeem Moghal, and Piali Sengupta for plasmids, Jim Rocca for help with NMR acquisition, Jodie Johnson for MS-MS analysis, Yousong Ding and Yi Zhang for help with Sybyl software, Steve Hagan, Gail Fanucci, and Zhanglong Liu for help with CD spectroscopy, and Yu Zhu for help with calculating CD spectra. We acknowledge the CGC, which is funded by the NIH Office of Research Infrastructure Programs (P40 OD010440), and the NemaGENETAG consortium for providing strains. This work was supported by funds to R.A.B. from the NIH (GM118775), the NSF (1555050), the Ellison Medical Foundation (AG-NS-0963-12), the Alfred P. Sloan Foundation (BR2014-071), and the National High Magnetic Field Laboratory, which is supported by NSF Cooperative Agreement No. DMR-1157490 and the State of Florida.

References

1. Omura S, Crump A. Ivermectin: panacea for resource-poor communities? Trends Parasitol. 2014; 30:445–455. [PubMed: 25130507]
2. Fischbach MA, Walsh CT. Assembly-line enzymology for polyketide and nonribosomal Peptide antibiotics: logic, machinery, and mechanisms. Chem Rev. 2006; 106:3468–3496. [PubMed: 16895337]
3. Castoe TA, Stephens T, Noonan BP, Calestani C. A novel group of type I polyketide synthases (PKS) in animals and the complex phylogenomics of PKSs. Gene. 2007; 392:47–58. [PubMed: 17207587]
4. Hojo M, et al. Unexpected link between polyketide synthase and calcium biomineralization. Zoological Letters. 2015; 1:1–16. [PubMed: 26605046]
5. O'Brien RV, Davis RW, Khosla C, Hillenmeyer ME. Computational identification and analysis of orphan assembly-line polyketide synthases. J Antibiot (Tokyo). 2014; 67:89–97. [PubMed: 24301183]
6. Wang H, Fewer DP, Holm L, Rouhiainen L, Sivonen K. Atlas of nonribosomal peptide and polyketide biosynthetic pathways reveals common occurrence of nonmodular enzymes. Proc Natl Acad Sci U S A. 2014; 111:9259–9264. [PubMed: 24927540]
7. Gowda H, et al. Interactive XCMS Online: simplifying advanced metabolomic data processing and subsequent statistical analyses. Anal Chem. 2014; 86:6931–6939. [PubMed: 24934772]
8. Nass R, Hamza I. The nematode *C. elegans* as an animal model to explore toxicology in vivo: solid and axenic growth culture conditions and compound exposure parameters. Curr Protoc Toxicol. 2007; Chapter 1(Unit 1):9. [PubMed: 20922756]
9. Bhushan R, Brückner H. Marfey's reagent for chiral amino acid analysis: a review. Amino Acids. 2004; 27:231–247. [PubMed: 15503232]
10. Kwan DH, Schulz F. The stereochemistry of complex polyketide biosynthesis by modular polyketide synthases. Molecules. 2011; 16:6092–6115. [PubMed: 21775938]

11. Aron ZD, Dorrestein PC, Blackhall JR, Kelleher NL, Walsh CT. Characterization of a new tailoring domain in polyketide biogenesis: the amine transferase domain of MycA in the mycosubtilin gene cluster. J Am Chem Soc. 2005; 127:14986–14987. [PubMed: 16248612]
12. Rottig M, et al. NRPSpredictor2--a web server for predicting NRPS adenylation domain specificity. Nucleic Acids Res. 2011; 39:W362–367. [PubMed: 21558170]
13. Du L, Lou L. PKS and NRPS release mechanisms. Nat Prod Rep. 2010; 27:255–278. [PubMed: 20111804]
14. Forrester WC, Perens E, Zallen JA, Garriga G. Identification of *Caenorhabditis elegans* genes required for neuronal differentiation and migration. Genetics. 1998; 148:151–165. [PubMed: 9475729]
15. Baugh LR. To grow or not to grow: nutritional control of development during *Caenorhabditis elegans* L1 arrest. Genetics. 2013; 194:539–555. [PubMed: 23824969]
16. Fukuyama M, Kontani K, Katada T, Rougvie AE. The *C elegans* Hypodermis Couples Progenitor Cell Quiescence to the Dietary State. Curr Biol. 2015; 25:1241–1248. [PubMed: 25891400]
17. Lee BH, Ashrafi K. A TRPV channel modulates *C elegans* neurosecretion, larval starvation survival, and adult lifespan. PLoS Genet. 2008; 4:e1000213. [PubMed: 18846209]
18. Chen Y, Baugh LR. *Ins-4* and *daf-28* function redundantly to regulate *C elegans* L1 arrest. Dev Biol. 2014; 394:314–326. [PubMed: 25128585]
19. Artyukhin AB, Schroeder FC, Avery L. Density dependence in *Caenorhabditis* larval starvation. Sci Rep. 2013; 3:2777. [PubMed: 24071624]
20. Frand AR, Russel S, Ruvkun G. Functional genomic analysis of *C elegans* molting. PLoS Biol. 2005; 3:e312. [PubMed: 16122351]
21. Baugh LR, Sternberg PW. DAF-16/FOXO regulates transcription of *cki-1*/Cip/Kip and repression of *lin-4* during *C elegans* L1 arrest. Curr Biol. 2006; 16:780–785. [PubMed: 16631585]
22. Ramaswamy V, et al. Development of a ^{13}C-optimized 1.5-mm high temperature superconducting NMR probe. J Magn Reson. 2013; 235:58–65. [PubMed: 23969086]
23. Chambers MC, et al. A cross-platform toolkit for mass spectrometry and proteomics. Nat Biotechnol. 2012; 30:918–920. [PubMed: 23051804]
24. Butcher RA, Fujita M, Schroeder FC, Clardy J. Small-molecule pheromones that control dauer development in *Caenorhabditis elegans*. Nat Chem Biol. 2007; 3:420–422. [PubMed: 17558398]
25. Modzelewska K, Lauritzen A, Hasenoeder S, Brown L, Georgiou J, Moghal N. Neurons refine the *Caenorhabditis elegans* body plan by directing axial patterning by Wnts. PLoS Biol. 2013; 11:e1001465. [PubMed: 23319891]
26. Zhang X, et al. Acyl-CoA oxidase complexes control the chemical message produced by *Caenorhabditis elegans*. Proc Natl Acad Sci U S A. 2015; 112:3955–3960. [PubMed: 25775534]
27. Ritter AD, et al. Complex expression dynamics and robustness in *C elegans* insulin networks. Genome Res. 2013; 23:954–965. [PubMed: 23539137]
28. Livak KJ, Schmittgen TD. Analysis of relative gene expression data using real-time quantitative PCR and the $2^{-\Delta\Delta C}{}_{T}$ Method. Methods. 2001; 25:402–408. [PubMed: 11846609]
29. Zhang X, Zabinsky R, Teng Y, Cui M, Han M. microRNAs play critical roles in the survival and recovery of *Caenorhabditis elegans* from starvation-induced L1 diapause. Proc Natl Acad Sci U S A. 2011; 108:17997–18002. [PubMed: 22011579]
30. Tamura K, Stecher G, Peterson D, Filipski A, Kumar S. MEGA6: Molecular Evolutionary Genetics Analysis version 6.0. Mol Biol Evol. 2013; 30:2725–2729. [PubMed: 24132122]
31. Weber T, et al. antiSMASH 3.0-a comprehensive resource for the genome mining of biosynthetic gene clusters. Nucleic Acids Res. 2015; 43:W237–243. [PubMed: 25948579]

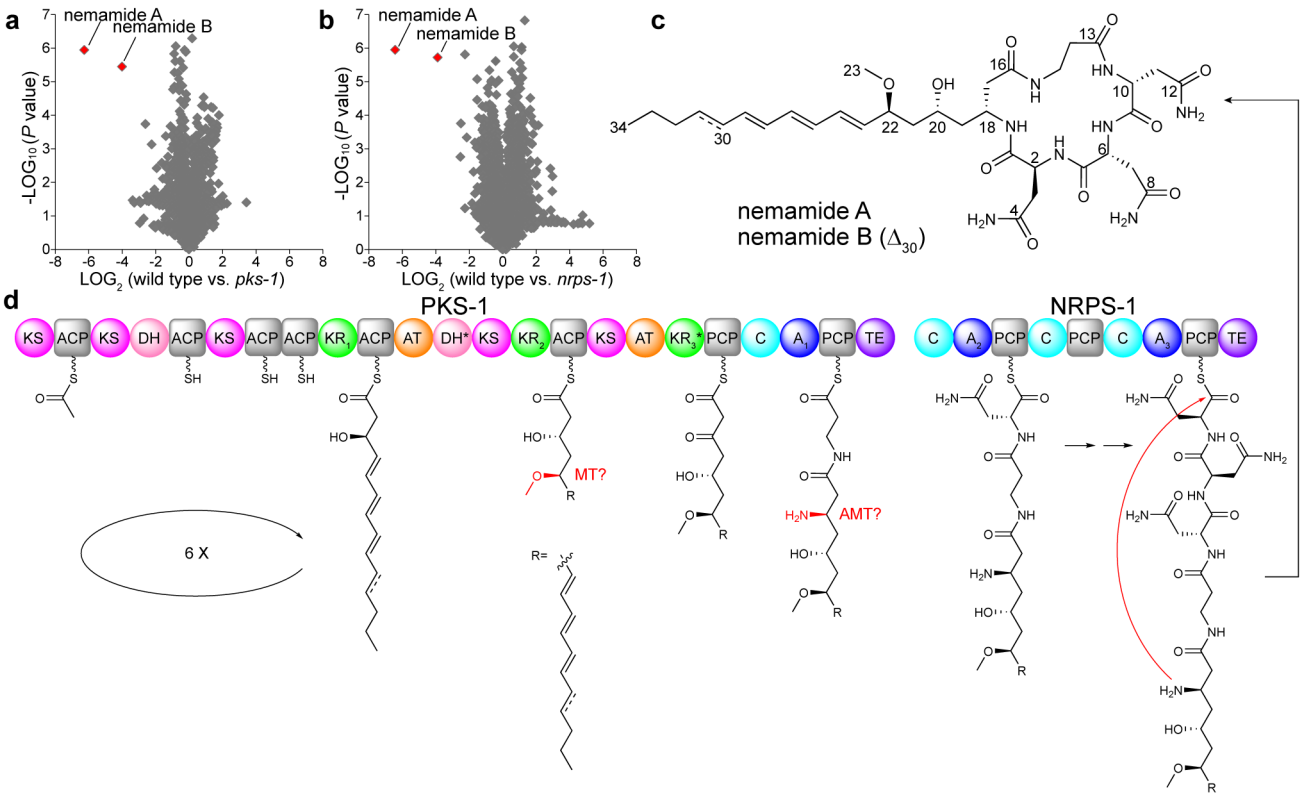

Figure 1. Discovery and biosynthesis of the nemamides

(**a**,**b**) Comparison of average peak areas for metabolite features in wild-type worms versus *pks-1* mutant worms (**a**) and in wild-type worms versus *nrps-1* mutant worms (**b**), with nemamide A and B highlighted in red. In **a** and **b**, extracts from three separate cultures were analyzed for each strain, and *P* values were calculated in XCMS using a Welch's t-test. (**c**) Chemical structures of nemamide A and B. (**d**) Proposed biosynthetic assembly line for the nemamides. Domain abbreviations: acyl transferase (AT), acyl carrier protein (ACP), ketosynthase (KS), ketoreductase (KR), dehydratase (DH), methyltransferase (MT), aminotransferase (AMT), adenylation (A), peptidyl carrier protein (PCP), condensation (C), and thioesterase (TE). Domains labeled with an asterisk are predicted to be inactive based on the nemamide structures. The KR and A domains are labeled with numbers for further discussion in Supplementary Figure 13 and Supplementary Table 4. KR_1 is predicted to be B-type, while KR_2 and KR_3 are neither A- nor B-type (Supplementary Fig. 13). Given that the nemamides contain four amino acids and that PKS-1 and NRPS-1 have only three A domains, A_2 may act twice to incorporate two Asn residues.

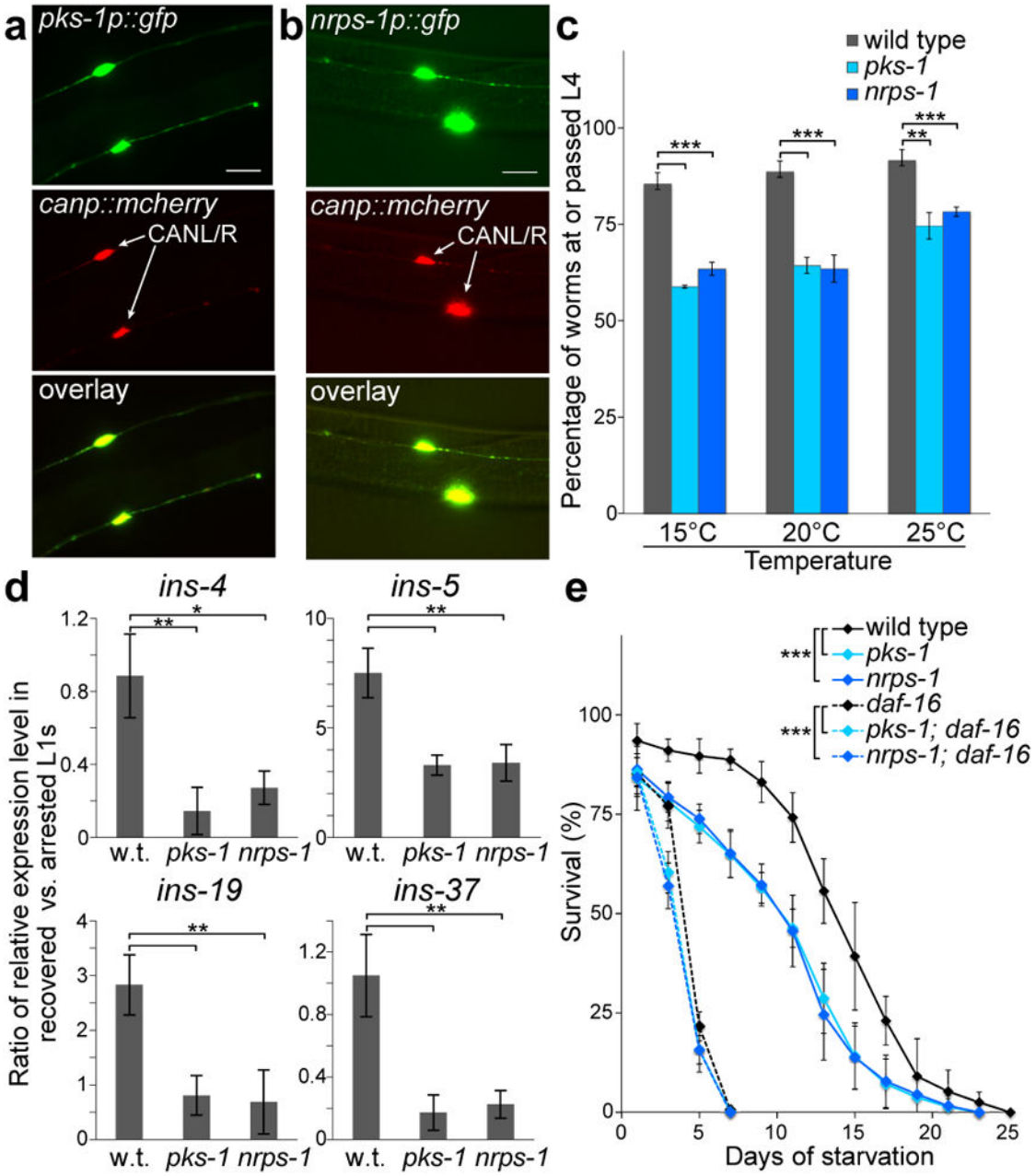

Figure 2. Site of expression and biological role of the nemamides

(**a,b**) Expression of the transcriptional reporters *pks-1p::gfp* (**a**) or *nrps-1p::gfp* (**b**), as well as *canp::mcherry* (marker for CAN neurons), in transgenic worms. Scale bar, 20 μm. We obtained similar results for *pks-1p::gfp-pest* and *nrps-1p::gfp-pest* reporters, in which GFP undergoes rapid turnover[20]. (**c**) Recovery of arrested L1s and development to the L4 stage for wild-type, *pks-1*, and *nrps-1* worms at different temperatures. (**d**) Expression of specific insulins in recovered versus arrested wild-type, *pks-1*, and *nrps-1* L1s, as determined by qRT-PCR. (**e**) Survival of wild-type, *pks-1*, and *nrps-1* arrested L1s over time. The insulin/IGF-1 pathway controls L1 survival in a manner dependent on the downstream *daf-16/foxo* transcription factor[15,21]. The poor survival of *daf-16/foxo (mu86 null)* was slightly enhanced

by the *pks-1* and *nrps-1* mutations. Mean survival (days ± SE): 14.3±0.2 for wild type, 11.3±0.3 for *pks-1*, 11.0±0.3 for *nrps-1*, 4.4±0.1 for *daf-16*, 3.7±0.1 for *pks-1; daf-16*, and 3.5±0.1 for *nrps-1; daf-16*. In **c–e**, the data represent the mean ± SD of three independent experiments, and two-tailed, unpaired t-tests were applied (*$P \leq 0.05$, **$P \leq 0.01$, ***$P \leq 0.001$).